Hindawi Publishing Corporation
Journal of Nanomaterials
Volume 2012, Article ID 962073, 10 pages
doi:10.1155/2012/962073

Research Article

Morphological and Structural Studies of Titanate and Titania Nanostructured Materials Obtained after Heat Treatments of Hydrothermally Produced Layered Titanate

Mohd Hasmizam Razali,[1,2] Ahmad-Fauzi Mohd Noor,[1] Abdul Rahman Mohamed,[3] and Srimala Sreekantan[1]

[1] *School of Material and Mineral Resources Engineering, Engineering Campus, University of Science, Malaysia, Seri Ampangan, Nibong Tebal, 14300 Pulau Pinang, Malaysia*
[2] *Department of Chemical Sciences, Faculty of Science and Technology, Universiti Malaysia Terengganu, 21030 Kuala Terengganu, Malaysia*
[3] *School of Chemical Engineering, Engineering Campus, University of Science, Malaysia, Seri Ampangan, Nibong Tebal, 14300 Pulau Pinang, Malaysia*

Correspondence should be addressed to Ahmad-Fauzi Mohd Noor, afauzi@eng.usm.my

Received 18 June 2012; Revised 1 September 2012; Accepted 5 September 2012

Academic Editor: Renzhi Ma

Different types of titanate and titania nanostructured materials have been successfully synthesised and characterized using field emission scanning electron microscopy (FESEM), transmission electron microscopy (TEM), X-ray diffraction (XRD) and raman spectroscopy. Elemental analysis was determined by energy dispersive X-ray spectroscopy (EDX) analyzer while thermogravimetric-differential scanning calorimetry (TG-DSC) was used to determine thermal stability. In this study, we found that nanotubes were formed during the washing treatment stage with HCl and distilled water. When the pH of the washing solution was 12, sodium titanate nanotubes were obtained, while when the pH of the washing solution was 7, hydrogen titanate nanotubes were obtained. Sodium titanate nanotubes were thermally stable up to 500°C; however, at 700°C, the nanotubes structure transform to solid nanorods. Meanwhile, hydrogen titanate nanotubes decomposed to produce titania nanotubes after heat treatment at 300°C for 2 hours. At 500°C, the tubular structure broke to small segments due to destruction of the nanotube. Further heat treatment at 700°C, led to the destruction and collapse of the nanotubes structure produce titania nanoparticles.

1. Introduction

After years of evolutionary research on titanate and titania nanostructured material production, many technologies based on "bottom up" processes such as the sol-gel method [1–3], chemical vapour deposition [4], template method [5], anodic anodization method [6], and hydrothermal method [7] have been developed. However, from the viewpoint of their environmental impact and cost operation for large-scale production, the hydrothermal method offers the best option since this method is simple, inexpensive, and efficient for obtaining products with high purity in both phases and morphology.

The hydrothermal method, based on wet chemistry method, is a versatile heterogeneous chemical reaction in the presence of a solvent, aqueous or nonaqueous, conducted in steel pressure vessels called autoclaves with or without Teflon liners under controlled temperature and pressure [8]. The temperature and the amount of solution added to the autoclave largely determine the internal pressure produced. Under the hydrothermal condition, it is possible to grow nanostructured metal oxides by dissolution and crystallization, thereby creating a distinctive difference in their characteristics at the nanoscale level [8].

Even though the hydrothermal method has caught the interest of researchers to synthesize nanostructured titanate

and titania materials, particularly the nanotubes, somehow the formation mechanism of the nanotubes hydrothermally is still debatable. Furthermore, different crystal structures and compositions have been presented to describe the nanotubes structure. Therefore, it is very important to study the actual mechanism of nanotube formation and to determine at which stage the nanotubes structure was formed. This in turn will determine the composition and phase structure.

Based on previous studies, researchers claimed that the nanotubes are form either during the hydrothermal process or during washing treatment with HCl and distilled water. In 2005, Lim et al. [9] reported that the nanotubes of TiO_2 are formed during the hydrothermal process. During the hydrothermal process at high temperature, the sodium cations (Na^+) residing between the edge-shared (TiO_6) octahedral layers can be replaced gradually by H_2O molecules. The size of intercalated H_2O molecules is larger than that of Na^+ ions, hence the interlayer distance becomes enlarged, and the static interaction between neighboring (TiO_6) octahedral sheets is weakened. Subsequently, the layered titanate particles exfoliate to form nanosheets. To release strain energy, the nanosheets curl up from the edges to form TiO_2 nanotubes.

Later, Peng et al. [10] proposed in their study that during alkaline treatment, anatase titania nanoparticles undergo delamination in the alkali solution to produce single-layer TiO_2 sheets. The TiO_2 sheet is an unstable structure due to its high surface-to-volume ratio or high system energy. At low treatment temperature (lower than 170°C), TiO_2 sheets might fold up by epitaxial growth to form titania nanotubes. During further treatment at higher temperature (higher than 190°C), titania nanotubes can self-assemble into a bundle-like superstructure of titania nanotubes.

Other researchers like Wang et al. [11] also found that tubes structure was formed during the hydrothermal process. They reported that during the reaction process, titanium dioxide reacts with NaOH forming layered alkali titanate. These layered crystals are very thin and easily exfoliate into individual nanosheets that are highly anisotropic in two dimensions. At a high pressure of 2 bars and a high temperature of about 150°C, the layered structure would roll up into nanotubes due to surface tension.

Nakahira et al. [12] reported that in the primary stages of hydrothermal treatment, the nanosheet-like products (layered sodium titanate) were preferentially formed and, subsequently, their nanosheets were exfoliated from layered sodium titanate, curled, and scrolled to nanotubes. Thus, the sodium titanate nanotubes were formed during these hydrothermal treatments.

Kasuga et al. [13] found out that titania nanotubes were formed after washing with distilled water and HCl aqueous solution. Kasuga proposed that the NaOH treatment broke some surface Ti–O–Ti bonds of the raw material, forming Ti–O–Na and Ti–OH bonds in their place. The subsequent acid washing destroyed the surface activation leading to dehydration of the Ti-OH bonds allowing the formation of Ti–O–Ti bond and (Ti–O$\cdots$H–O–Ti). The Ti–OH bonds formed through this procedure were believed to form from the decreasing Ti bond distance on the sheet's surface during the dehydration process. A residual electrostatic repulsion from the Ti–O–Na bonds was believed to induce the ends of the formed sheet to connect, hence forming the tube structure of TiO_2.

Besides TiO_2 nanotubes, researchers also reported that the obtained nanotubes materials were in different crystal structures and compositions such as hydrogen trititanate ($H_2Ti_3O_7$) [14], tetratitanate ($H_2Ti_4O_9\cdot H_2O$) [15], lepidocrocite titanate $Na_xH_{2-x}Ti_3O_7$ [16], and $H_2Ti_2O_4(OH)_2$ [17]. Therefore, this study was embarked to evaluate the crystal structure and morphology of the products obtained after heat treatment of the as-synthesized samples at different pH values of washing solution. It can provide strong evidence about its original crystal structure and allow us to know when the nanotube structures were formed.

2. Methodology

2.1. Preparation. 2 grams of TiO_2 precursor powder (Merck) was dispersed in 10 M NaOH (100 mL) and was subjected to hydrothermal treatment at 150°C for 24 hours in autoclave. When the reaction was completed, the white solid was collected and divided to two parts. The first portion was washed with 0.1 M HCl (200 mL) followed by distilled water until a pH 12 of washing solution was obtained. Meanwhile, a second portion was washed with 0.1 M HCl (200 ml) followed by distilled water until a pH 7 of washing solution was obtained. Then, the white solid was separated and collected from both solutions and subsequently dried at 80°C for 24 hours. After drying, the obtained powder from pH 12 and pH 7 washing solution was named as-synthesized samples A and B, respectively. Subsequently, both samples were heated at 300°C, 500°C, and 700°C for 2 hours in the air.

2.2. Characterization. Energy-dispersive X-ray spectroscopy (EDX) analyzer was used for elemental analysis in the sample, while the morphology was studied using scanning electron microscope with GEMINI field emission (FESEM) and JOEL transmission electron microscope (TEM). X-ray powder diffraction (XRD) analysis was performed using a diffractometer D5000 Siemens kristalloflex with Cu K_α radiation ($\lambda = 1.54060$ Å). Scans were performed in the step of 0.2°/second over the range of 2θ from 20 up to 80°. Raman spectra were analysed using RENISHAW Invia Raman microscope and recorded in the range 100–1000 cm^{-1}. Thermal stability study of the sample was done using thermogravimetry and differential scanning calorimetry (TG-DSC) SDT Q600.

3. Results and Discussion

Figure S1 of the supplementary matrial avalible online at doi: 10.1155/2012/962073 shows the FESEM micrograph of the TiO_2 precursor, revealing agglomerated irregularly shaped particles containing Ti and O as indicated by EDX (Figure S3). On the other hand, spherical particles of the TiO_2

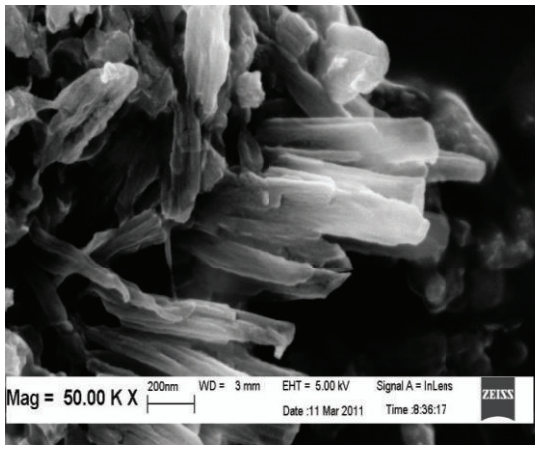

Figure 1: FESEM micrograph of $Na_2Ti_3O_7$.

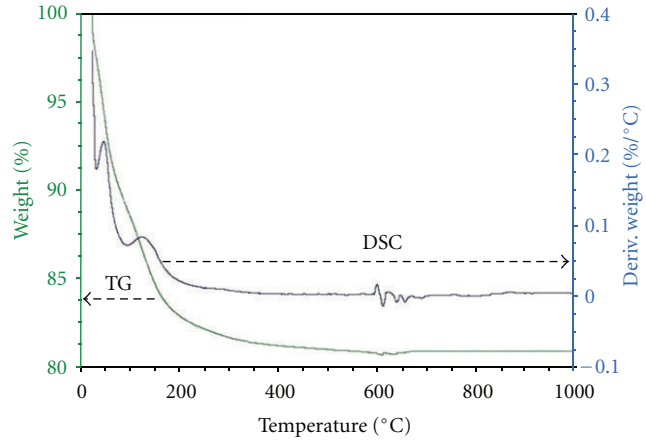

Figure 2: TG-DSC spectrum for the as-synthesised sample A.

Table 1: Sodium content in the sample.

Samples	Na (wt%)
Without washing	45.93
As-synthesised sample A	10.46
As-synthesised sample B	0.00

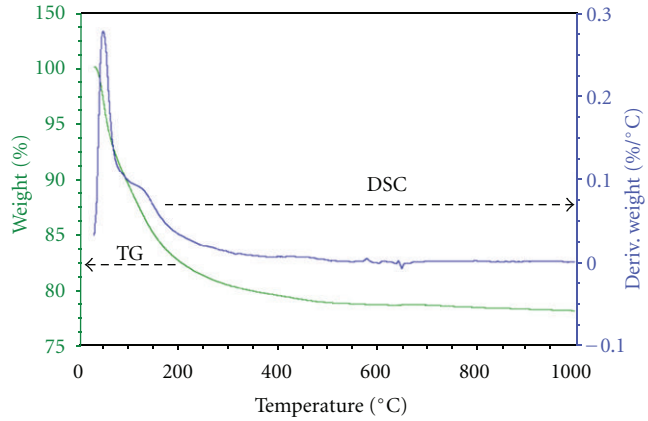

Figure 3: TG-DSC spectrum for the as-synthesised sample B.

precursor can be seen clearly in the TEM micrograph with the particle size being about 160 nm (Figure S2). During the hydrothermal treatment, the titanium dioxide precursor (TiO_2) reacts with NaOH forming a highly disordered phase of $Na_2Ti_3O_7$ which is present in the layered structure form [18]. TiO_2 is an amphoteric oxide it can react as an acid or base depending on the pH of the solution. Since the reaction was carried out in 10 M NaOH (high pH~14 and high basicity), TiO_2 acted as an acid to react with NaOH (alkaline) to produce layered titanate of $Na_2Ti_3O_7$ salt and water, H_2O, according to the following equation [18]:

$$3TiO_2 + 2NaOH \longrightarrow Na_2Ti_3O_7 + H_2O \quad (1)$$

The layered-like structure of $Na_2Ti_3O_7$ was shown in the FESEM micrograph (Figure 1) containing Na, Ti, and O as indicated by EDX (Figure S5).

After the hydrothermal treatment, the obtained product (layered titanate, $Na_2Ti_3O_7$) was washed with HCl (0.1 M) and distilled water. Washing plays an important role in controlling the amount of Na^+ ions remaining in the sample solution, thus influencing the bending of the layered titanate. Zhang et al. [19] stated that due to the imbalance of H^+ and Na^+ ion concentrations on the two different sides of the layered-like structure, excess surface energy and the layered-like structure bends to form nanotubes.

In this study, washing was carried out until the pHs of the washing solutions was 7 and 12, respectively, and this will influence the amount of sodium remaining in the samples. Hence, EDX analysis was carried out to investigate the presence of sodium in the samples because it is vital in determining the thermal stability, phase structure, and morphology of the synthesized nanostructured materials. For comparison, elemental analysis for the sample obtained after hydrothermal process (without washing) was performed and that sample was found to consist of 45.93 wt% of sodium (Table 1) (Figure S4). After washing till the pH 12, sodium content was found to be reduced to 10.46 wt% (as-synthesised sample A) (Table 1) (Figure S5). It was shown that about 35 wt% of sodium ions has been exchanged with hydrogen ions. Meanwhile, when the sample was completely washed, with the pH of washing solution equal to 7 (as-synthesised sample B), no more sodium was detected, which indicated that sodium ions were completely removed and exchanged with hydrogen ions during washing with HCl and distilled water (Table 1) (Figure S6).

Hydrogen cannot be detected by EDX, but nevertheless, theoretically, H^+ is extremely reactive chemically due to its very small size of only about 1/64,000th of the radius of a hydrogen atom and the fact that it exists as a free proton which makes it react immediately by exchange with Na^+. Based on the density functional theory, the sodium ion can be replaced by hydrogen ion although the $Na_2Ti_3O_7$ structure is very stable [19]. This is possible since the sodium ions are only weakly bonded to the negatively charged $Ti_3O_7^{2-}$ layers. While the Na–O bond length in $Na_2Ti_3O_7$ is above 2Å, the bond length of H–O in $H_2Ti_3O_7$ is about 1Å. Therefore, the

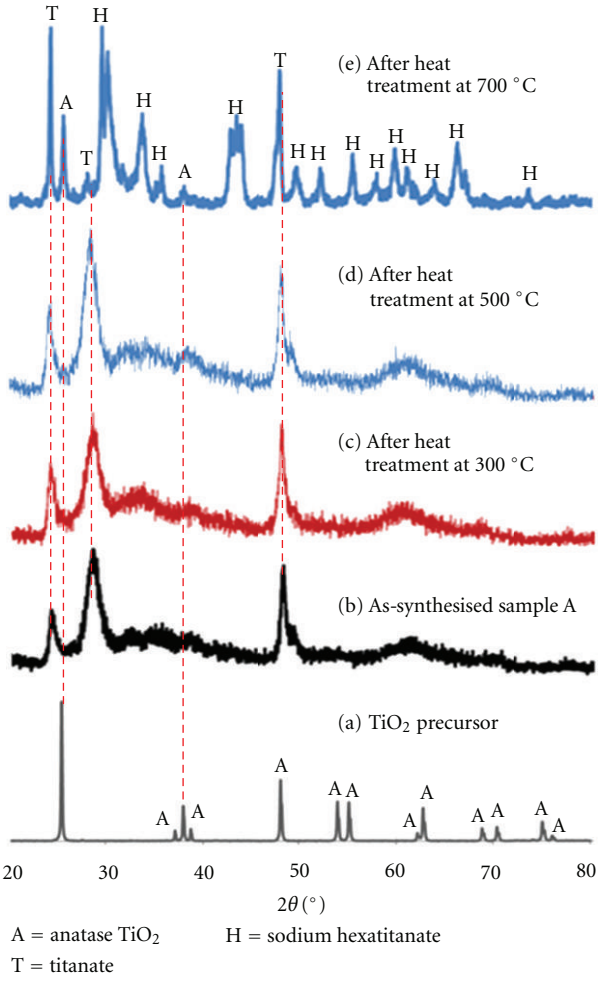

Figure 4: XRD patterns of (a) TiO_2 precursors, (b) as-synthesised sample A and after heat treatments at (c) 300°C, (d) 500°C, and (e) 700°C for 2 hours.

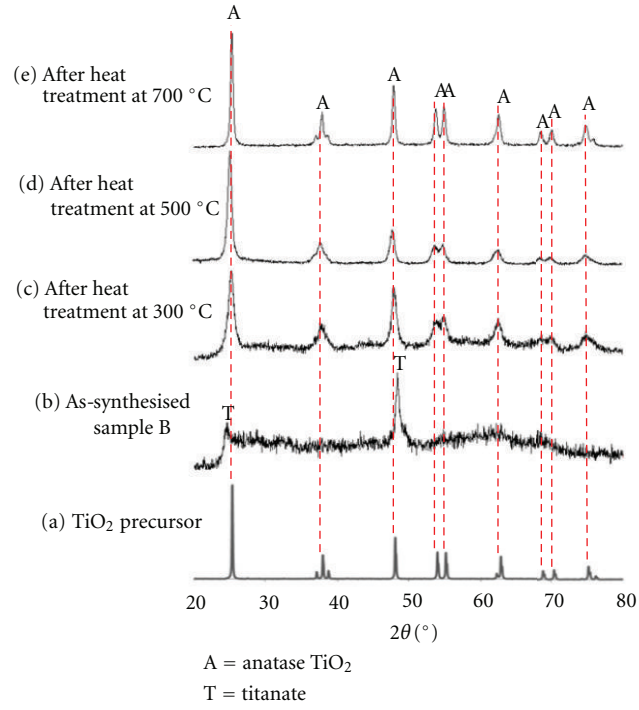

Figure 5: XRD patterns of (a) TiO_2 precursor, (b) as-synthesised sample B and after heat treatments at (c) 300°C, (d) 500°C, and (e) 700°C for 2 hours.

hydrogen ion exchange process is irreversible. Furthermore elution strength of H^+ is larger than Na^+; therefore, the ion exchange between H^+ and Na^+ is possible to occur according to the following equation.

Dissolution-crystallisation layered structure:

$$Na_2Ti_3O_7 \longrightarrow 2Na^+ + Ti_3O_7^{2-} \quad (2)$$

Ion exchanged during washing occurs as follows:

$$2Na^+ + Ti_3O_7^{2-} + H^+ + Cl^- \longrightarrow H^+ + Ti_3O_7^{2-} + 2Na^+ + Cl^- \quad (3)$$

Crystallisation for salt formation is as follows:

$$Na^+ + Cl^- \longrightarrow NaCl\ (\text{dissolved in an aqueous solution}) \quad (4)$$

Crystallisation for titanate formation is as follows:

$$2H^+ + Ti_3O_7^{2-} \longrightarrow H_2Ti_3O_7\ (\text{white precipitate in an aqueous solution}) \quad (5)$$

The ion exchange reaction occurred very fast as no electron pair was needed to be broken and the rate of the process is limited only by the rate at which ions can be diffused in and out of the exchanger structure. Thus, it was expected that the titanate product obtained in this study can be used as an ion exchanger due to the rapidity and efficiency of their actions. Furthermore, the ion exchange and structural properties of titanate allows for efficient ion mobility in the interstices and an open mesoporous structure for electrolyte diffusion. These features give rise to a high discharge/charge capability, high rate capability, and excellent stability, and this is one key requirement for lithium batteries.

In order to study the thermal stability of the titanate products, thermogravimetric and differential scanning calorimetry (TG-DSC) was performed in nitrogen atmosphere from room temperature to 1000°C, with heating rate of 5°C/min.

Both samples show almost similar TG curves (Figures 2 and 3), showing decrease in mass starting at room temperature until 700°C, with total mass loss of about 22%. In general, the weight loss between room temperature till 100°C is due to the removal of adsorbed water from the surface. When the temperature is further increased up to 200°C, the intercalated water molecules such as dissociated molecular H_2O, physisorbed molecular H_2O and chemisorbed molecular H_2O are removed. This also includes Ti–OH bonds within tubular structure [20]. Subsequently, a small weight

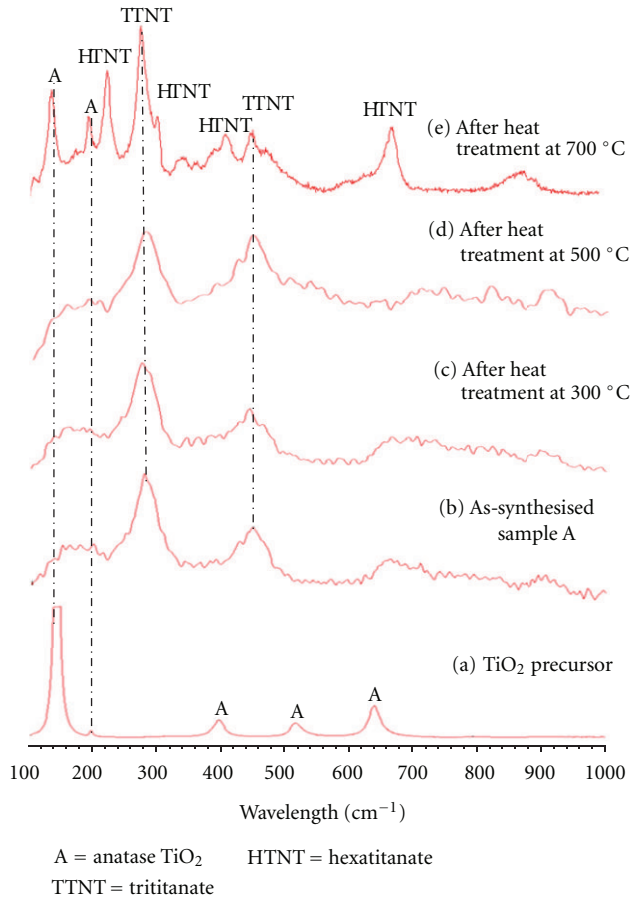

Figure 6: Raman spectra of (a) TiO_2 precursor (b) as-synthesised sample A and after heat treatments at (c) 300°C, (d) 500°C, and (e) 700°C for 2 hours.

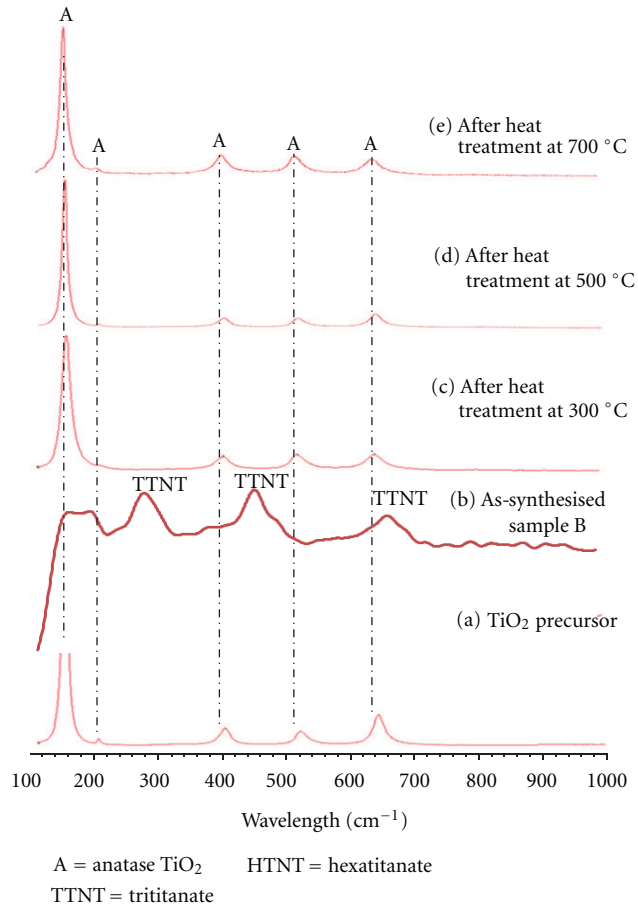

Figure 7: Raman spectra of (a) TiO_2 precursors, (b) as-synthesised sample B and after heat treatments at (c) 300°C, (d) 500°C, and (e) 700°C for 2 hours.

loss in the region of 200–700°C was due to the dehydration of titanate nanotubes and transformation of phase structure.

On the other hand, the DSC graphs in Figures 2 and 3 show larger two endothermic peaks at 70°C and 150°C which are characteristics for the evaporation of different states of adsorbed water molecules. Few smaller endothermic and exothermic peaks at 600–700°C are attributed to the transformation of morphology and phase crystal structures.

X-ray diffraction was carried out to study the crystal structure of the samples and effect of heat treatment on the crystal structure. The X-ray diffractogram patterns of the as-synthesized sample A is shown in Figure 4. The TiO_2 precursor shows a series of sharp and narrow peaks, the highest being 101 at 25.27°, which is characteristic of the anatase TiO_2 phase structure (Figure 4(a)). Meanwhile, XRD pattern of as-synthesised sample A and after heat treatment at 300°C and 500°C shows the presence of similar peaks which are identical to sodium titanate [21] (Figures 4(b), 4(c), and 4(d)). Similar diffraction peaks suggesting the maintenance of the crystallographic and morphological structure up to 500°C and this could be ascribed to the interlayer spacing typical for one-dimensional titanate structure [22].

After 700°C heat treatment, emergence of new sharp and narrow peaks took place indicating that the crystallinity of the sample is increased. These new peaks can be assigned to sodium hexatitanate and titania anatase (Figure 4(e)). The presence of sodium hexatitanate phase in the thermal products is a crucial phenomenon in understanding the structural properties of titanate nanostructures. It seems that at higher temperatures sodium titanates undergo a dimerization-like process leading to the formation of sodium hexatitanates. The basic difference in the structures of sodium trititanates and sodium hexatitanates is that the former presents a lamellar structure with $Ti_3O_7^{2-}$ corrugated layers and two interlamellar Na^+ ions [23]. Previously, Sauvet et al. [24] proposed that at higher temperatures sodium trititanates tend to fuse and the formation of $Na_2Ti_6O_{13}$ is the result of the "dimerization-like" process of $Na_2Ti_3O_7$. The presence of $Na_2Ti_6O_{13}$ in the thermal products can be considered as strong evidence that the structure and composition of as-synthesised sample A are very similar to $Na_2Ti_3O_7$ and a general formula may be assigned as $Na_{2-x}H_xTi_3O_7$ due to some of the Na^+ being exchanged with H^+ during washing treatment.

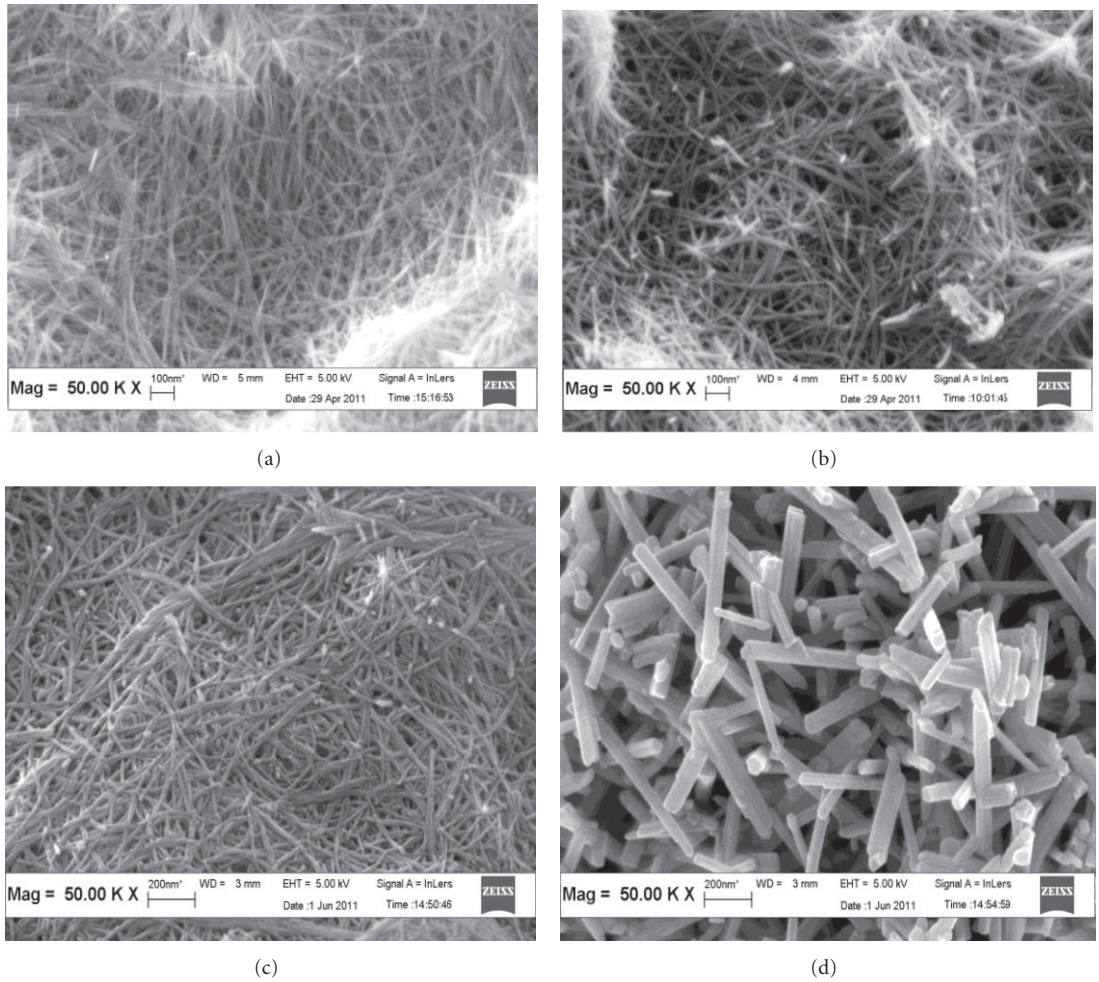

Figure 8: FESEM micrographs of (a) as-synthesized sample A and after heat treatments at (b) 300°C, (c) 500°C, and (d) 700°C for 2 hours.

Figure 5 presents the XRD patterns of as-synthesized sample B and its derivatives obtained at different temperatures as well-TiO_2 precursor for comparison. The TiO_2 precursor shows the existence of a series of sharp and narrow peaks which is characteristic of the anatase TiO_2 phase structure (Figure 5(a)). Meanwhile, XRD pattern of as-synthesized sample B (Figure 5(b)) is identical to hydrogen titanate, ($H_2Ti_3O_7$) [25]. For the samples after heat treatment at 300°C, 500°C, and 700°C (Figures 5(c), 5(d), and 5(e)), they show similar peaks which are assigned to TiO_2 anatase, but an increase in degree of crystallinity.

From the XRD analysis, it may be inferred that the composition and structure of the as-synthesised sample B is very similar to layered protonic titanate with a general formula that may be assigned as $H_2Ti_3O_7$. After heat treatment at 300°C or at higher temperature (≤700°C) for 2 hours, $H_2Ti_3O_7$ decomposes to produce TiO_2 with anatase phase according to the following equation [25]:

$$H_2Ti_3O_7 \longrightarrow 3TiO_2 + H_2O \quad (6)$$

It has been recognized that anatase TiO_2 is preferred because of its high photocatalytic activity, since it has a more negative conduction band edge potential (higher potential energy of photogenerated electrons). Anatase TiO_2 also has strong photoinduced redox power, thus it could be a superior photocatalytic material for purification and disinfection of water and air, as well as remediation of hazardous waste [26]. Furthermore, the with high surface area of nanostructured TiO_2 anatase increases the rate of a photocatalytic reaction, due to the presence of more active sites. The hollow structure of nanotubes can also potentially enhance electron percolation and light conversion, as well as the improved ion diffusion at the semiconductor photocatalyst-electrolyte interface [27, 28]. Therefore, synthesized nanostructured TiO_2 nanotubes in this study could potentially contribute to a high performance photocatalyst.

Further characterization was employed using raman spectroscopy. According to the factor group analysis, anatase TiO_2 has six raman active modes (A1g + 2B1g + 3Eg) [29]. Previously, Ohsaka et al. [30] studied the raman spectrum of an anatase TiO_2 single crystal and they identified six peaks which appeared at 144 cm^{-1} (Eg), 197 cm^{-1} (Eg), 399 cm^{-1} (B1g), 513 cm^{-1} (A1g), 519 cm^{-1} (B1g), and 639 cm^{-1} (Eg). In this study, fives peaks at 143 cm^{-1} (Eg), 197 cm^{-1} (Eg),

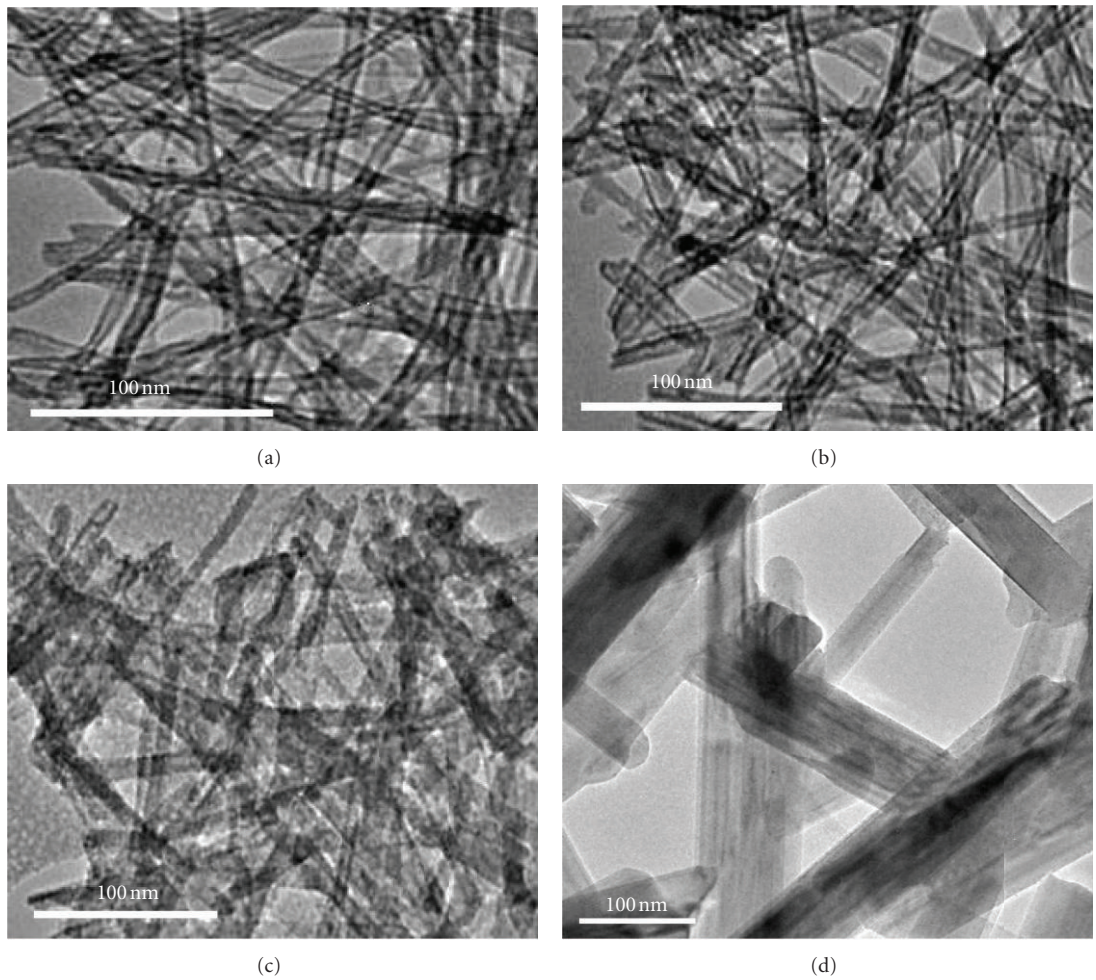

Figure 9: TEM micrographs of (a) as-synthesized sample A and after heat treatments at (b) 300°C, (c) 500°C, and (d) 700°C for 2 hours.

396 cm^{-1} (B1g), 516 cm^{-1} (A1g/B1g), and 639 cm^{-1} (Eg) were traced for the TiO_2 precursor (Figure 6(a)). According to Bergeret al. [31], the strongest peak at 143 cm^{-1} was attributed to the external vibration of the anatase structure, therefore it could be concluded that TiO_2 precursor is an anatase phase. This finding is in agreement with the XRD result, which showed that TiO_2 precursor is in anatase phase. In contrast, for as-synthesized sample A (Figure 6(b)) and after heat treatment at 300°C and 500°C for 2 hours (Figures 6(c) and 6(d)) peaks at only about 280 cm^{-1} and 446 cm^{-1} were observed. The broad peak at 280 cm^{-1} is assigned to the characteristic phonon mode of titanate structure [32], while the peak at 446 cm^{-1} is assigned to the Ti–O bending vibration involving six coordinated titanium atoms and three coordinated oxygen atoms in the layered titanate structure [29]. After heat treatment at 700°C, peaks at 280 cm^{-1} and 446 cm^{-1} can still be observed and a few new peaks appeared at about 135 cm^{-1}, 222 cm^{-1}, 405 cm^{-1}, 449 cm^{-1}, 630 cm^{-1} and 673 cm^{-1} (Figure 6(e)) suggesting that the presence of anatase of TiO_2 and hexatitanate structures.

On the other hand, the as-synthesized sample B showed the presence of three peaks at about 280 cm^{-1}, 446 cm^{-1}, and 664 cm^{-1} (Figure 7(b)). As reported previously, the broad peak at 280 cm^{-1} is assigned to the characteristic phonon mode of titanate nanotube structures [29] and the peak at 446 cm^{-1} is belongs to the Ti–O bending vibration involving six coordinated titanium atoms and three coordinated oxygen atom in layered titanate [31]. Meanwhile, the peak at 664 cm^{-1} is due to the Ti–O–H vibration [32]. Therefore, it could be concluded that as-synthesized sample B is $H_2Ti_3O_7$, which confirms the XRD result. After heat treatment at 300°C, 500°C, and 700°C for 2 hours, similar raman spectra (Figures 7(c), 7(d), and 7(e)) with TiO_2 precursor (Figure 7(a)) were observed, indicating that they are also TiO_2 in anatase phase.

The results obtained in this study clearly indicate that the structure of as-synthesised samples A (solid powder obtained after drying at 80°C for 24 h of white solid collected from pH 12 of washing solution) and as-synthesised sample B (solid powder obtained after drying at 80°C for 24 h of white solid collected from pH 7 of washing solution) are $Na_{2-x}H_xTi_3O_7$ and $H_2Ti_3O_7$, respectively.

Surface morphology of the samples was observed using FESEM and TEM. The FESEM micrographs of as-synthesized sample A revealed the formation of a hair-like structure with ±10 nm in diameter (Figure 8(a)).

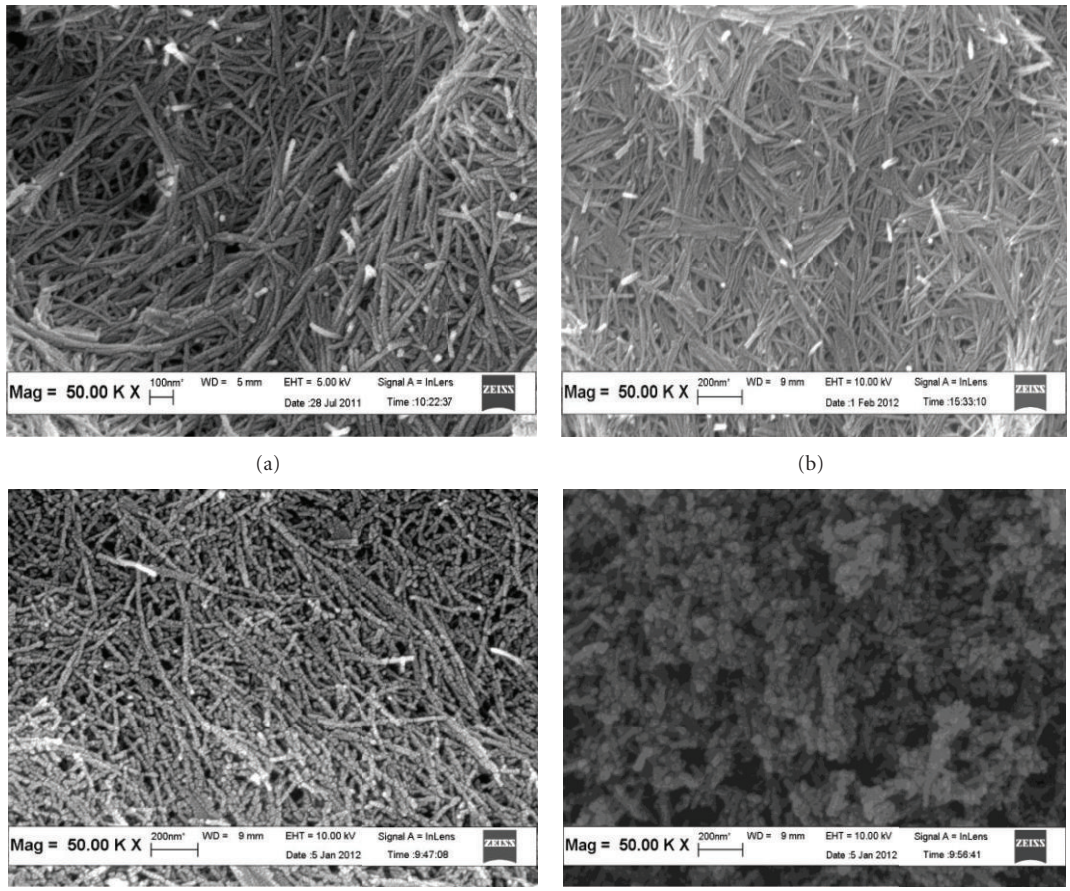

Figure 10: FESEM micrographs of (a) as-synthesised sample B and after heat treatments at (b) 300°C, (c) 500°C, and (d) 700°C for 2 hours.

Further observation with TEM showed the existence of a hollow structure inside the TiO_2 tubule indicating that nanotubes structures were obtained (Figure 9(a)). The inner and outer diameters of nanotubes are about 4 nm and 10 nm, respectively. After heat treatment at 300 and 500°C for 2 hours (Figures 8(b), 9(b), 8(c), and 9(c)), the samples still showed similar surface morphology with the as-synthesized sample, and thus revealing that there were no great influences on surface morphology of the nanotube structure at low annealing temperature (≤500°C). This indicated that the nanotube structure of as-synthesised sample A was thermally stable up to 500°C. However, when the annealing temperature was increased to 700°C, the nanotube structure had completely transformed to nanorods. The nanorod (nonhollow structure) with ±65 nm diameter were formed due to the mobilizations of dissolved Na^+ into the nanotubes inner channel (as well as the boundary pores among nanotubes) and then recrystallized to form nanorods (Figures 8(d) and 9(d)). The existence of sodium in the as-synthesised sample A was shown previously by EDX analysis.

As-synthesised sample B also shows the presence of a hair-like tubular structure (±10 nm in diameter) (Figure 10(a)) with the existence of a hollow space inside the tubular structure (±4 nm in diameter) (Figure 11(a)). Thus, the nanotubes with about ±4 nm inner and ±10 nm outer diameters were obtained. After heat treatment at 300°C for 2 hours, there was no significant influence on morphology of the material (Figure 10(b)). The nanotubes preserve their shape with their inner diameter being almost similar; however, their outer diameter increases up to 12 nm (Figure 11(b)), due to the dehydration of intralayered OH groups [33]. Surprisingly, at 500°C heat treatment, the morphology of the material was affected significantly. The tubular structures were broken to small segments due to destruction of the nanotubes. However, frames of the tubular structures were still visible (Figures 10(c) and 11(c)). When the heating temperature was increased to 700°C, the nanotube structure was completely destroyed and the individual tubes had formed into nanoparticle structures with particle size around 20 nm (Figures 10(d) and 11(d)). This was probably a result of dehydration of interlayered OH groups which induced the change of the crystalline structure and destroyed the nanotubes structure to produce nanoparticles, when the temperature of heat treatment was higher [33, 34].

The absence of the Na^+ in the as-synthesised sample B would cause the tube structure to be easily destroyed even after heat treatment at 500°C. Sodium ion was reported to play an important role in pinning adjacent layers, thus

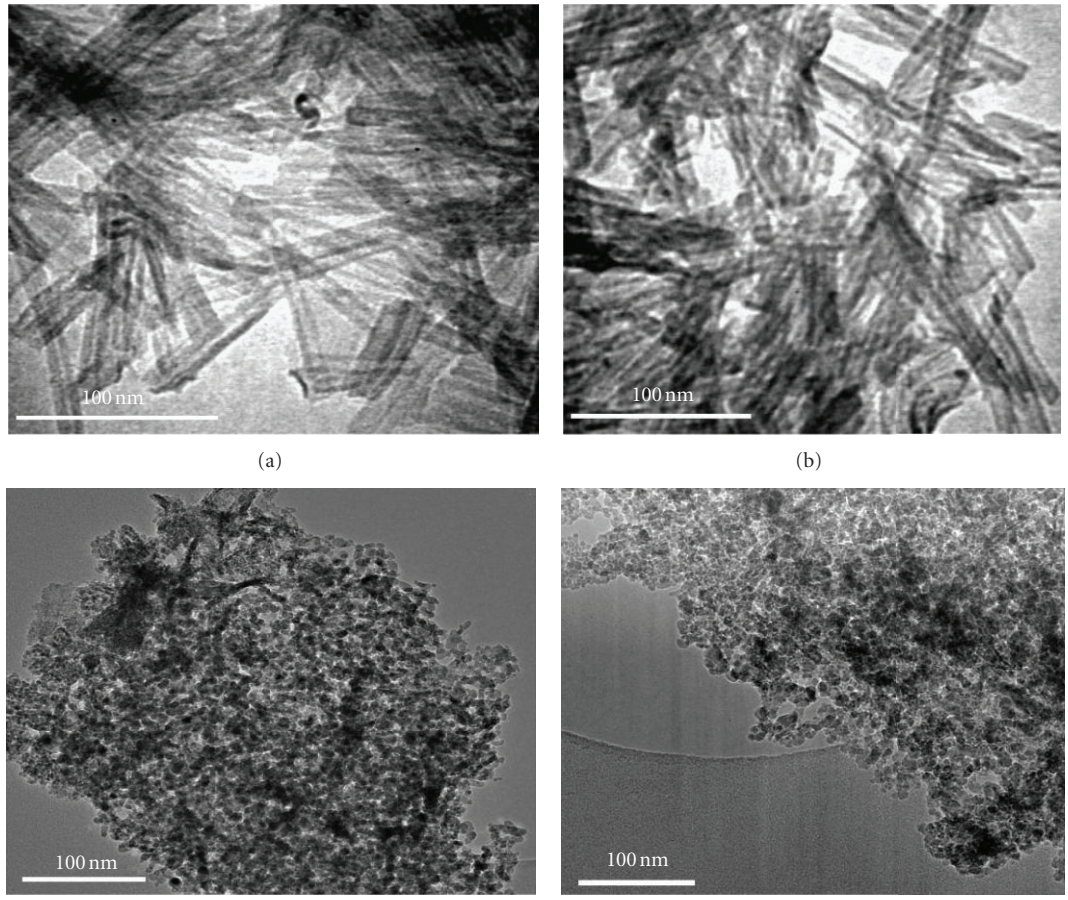

Figure 11: TEM micrographs of (a) as-synthesised sample B and after heat treatments at (b) 300°C, (c) 500°C, and (d) 700°C for 2 hours.

stabilizing the layered structure and tubular morphology [35].

4. Conclusion

Upon hydrothermal treatment of TiO_2 in NaOH, a disordered phase with a layered structure was formed. This disordered layered structured phase transformed into titanate nanotubes after being washed with HCl and distilled. When the pH of washing solution was 12, sodium titanate nanotube was obtained. The obtained nanotubes were thermally stable up to 500°C; however, at 700°C heating treatment nanotubes transformed to the titanate nanorods; while when the pH of washing solution was 7, hydrogen titanate nanotubes were obtained. After heat treatment at 300°C for 2 hours, hydrogen titanate nanotubes decomposed to produce titania nanotubes. After further heat treatment at 500°C, the tubular structure broke to small segments due to destruction of nanotube and, at 700°C, nanotube structure was totally destroyed and subsequently transformed to nanoparticle. Nanoparticles and nanotubes of titania obtained in this study have an anatase phase which is expected to be a high performance photocatalyst.

Acknowledgments

The authors are grateful to Universiti Sains Malaysia (USM) for providing the facilities to carry out this project. The authors would also like to thank Universiti Malaysia Terengganu (UMT) and the Ministry of Higher Education of Malaysia (MOHE) for their financial support.

References

[1] T. Sugimoto, X. Zhou, and A. Muramatsu, "Synthesis of uniform anatase TiO_2 nanoparticles by gel-sol method: 4. Shape control," *Journal of Colloid and Interface Science*, vol. 259, no. 1, pp. 53–61, 2003.

[2] C. Su, B. Y. Hong, and C. M. Tseng, "Sol-gel preparation and photocatalysis of titanium dioxide," *Catalysis Today*, vol. 96, no. 3, pp. 119–126, 2004.

[3] T. Sugimoto, X. Zhou, and A. Muramatsu, "Synthesis of uniform anatase TiO_2 nanoparticles by gel-sol method: 1. Solution chemistry of $Ti(OH)_n(4 - n)+$ complexes," *Journal of Colloid and Interface Science*, vol. 252, no. 2, pp. 339–346, 2002.

[4] T. Maekawa, K. Kurosaki, T. Tanaka, and S. Yamanaka, "Thermal conductivity of titanium dioxide films grown by metal-organic chemical vapor deposition," *Surface and Coatings Technology*, vol. 202, no. 13, pp. 3067–3071, 2008.

[5] J. H. Lee, I. C. Leu, M. C. Hsu, Y. W. Chung, and M. H. Hon, "Fabrication of aligned TiO_2 one-dimensional nanostructured arrays using a one-step templating solution approach," *Journal of Physical Chemistry B*, vol. 109, no. 27, pp. 13056–13059, 2005.

[6] N. R. De Tacconi, C. R. Chenthamarakshan, G. Yogeeswaran et al., "Nanoporous TiO_2 and WO3 films by anodization of titanium and tungsten substrates: influence of process variables on morphology and photoelectrochemical response," *Journal of Physical Chemistry B*, vol. 110, no. 50, pp. 25347–25355, 2006.

[7] D. S. Kim and S.Y. Kwak, "The hydrothermal synthesis of mesoporous TiO_2 with high crystallinity, thermal stability, large surface area, and enhanced photocatalytic activity," *Applied Catalysis A*, vol. 323, pp. 110–118, 2007.

[8] K. Byrappa and M. Yoshimura, *Handbook of Hydrothermal Technology—A Technology for Crystal Growth and Materials Processing*, Noyes, Park Ridge, NJ, USA, 2001.

[9] S. H. Lim, J. Luo, Z. Zhong, W. Ji, and J. Lin, "Room-temperature hydrogen uptake by TiO_2 nanotubes," *Inorganic Chemistry*, vol. 44, no. 12, pp. 4124–4126, 2005.

[10] H. Peng, G. Li, and Z. Zhang, "Synthesis of bundle-like structure of titania nanotubes," *Materials Letters*, vol. 59, no. 10, pp. 1142–1145, 2005.

[11] D. Wang, F. Zhou, Y. Liu, and W. Liu, "Synthesis and characterization of anatase TiO_2 nanotubes with uniform diameter from titanium powder," *Materials Letters*, vol. 62, no. 12-13, pp. 1819–1822, 2008.

[12] A. Nakahira, T. Kubo, and C. Numako, "Formation mechanism of TiO_2-derived titanate nanotubes prepared by the hydrothermal process," *Inorganic Chemistry*, vol. 49, no. 13, pp. 5845–5852, 2010.

[13] T. Kasuga, M. Hiramatsu, A. Hoson, T. Sekino, and K. Niihara, "Formation of titanium oxide nanotube," *Langmuir*, vol. 14, no. 12, pp. 3160–3163, 1998.

[14] Q. Chen, G. H. Du, S. Zhang, and L. M. Peng, "The structure of trititanate nanotubes," *Acta Crystallographica Section B*, vol. 58, no. 4, pp. 587–593, 2002.

[15] A. Nakahira, W. Kato, M. Tamai, T. Isshiki, K. Nishio, and H. Aritani, "Synthesis of nanotube from a layered $H_2Ti_4O_9 \cdot {}_7H_2O$ in a hydrothermal treatment using various titania sources," *Journal of Materials Science*, vol. 39, no. 13, pp. 4239–4245, 2004.

[16] M. Qamar, C. R. Yoon, H. J. Oh et al., "Effect of post treatments on the structure and thermal stability of titanate nanotubes," *Nanotechnology*, vol. 17, no. 24, pp. 5922–5929, 2006.

[17] M. Zhang, Z. S. Jin, J. J. Yung, and Z. Zhang, "Effect of annealing temperature on morphology, structure and photocatalytic behavior of nanotubed $H_2Ti_2O_4(OH)_2$," *Journal of Molecular Catalysis A*, vol. 217, pp. 203–210, 2004.

[18] Q. Chen, W. Z. Zhou, G. H. Du, and L. M. Peng, "Tritanate nanotubes made via a single alkali treatment," *Advanced Materials*, vol. 14, pp. 1208–1211, 2002.

[19] S. Zhang, L. M. Peng, Q. Chen, G. H. Du, G. Dawson, and W. Z. Zhou, "Formation Mechanism of $H_2Ti_3O_7$ Nanotubes," *Physical Review Letters*, vol. 91, Article ID 256103, 2003.

[20] L. Qian, Z. L. Du, S. Y. Yang, and Z. S. Yin, "Raman-study of titania nanotube by soft chemical-process," *Journal of Molecular Structure*, vol. 749, pp. 103–107, 2005.

[21] Y. Lan, X. P. Gao, H. Y. Zhu et al., "Titanate nanotubes and nanorods prepared from rutile powder," *Advanced Functional Materials*, vol. 15, no. 8, pp. 1310–1318, 2005.

[22] S. Ribbens, V. Meynen, G. V. Tendeloo et al., "Development of photocatalytic efficient Ti-based nanotubes and nanoribbons by conventional and microwave assisted synthesis strategies," *Microporous and Mesoporous Materials*, vol. 114, no. 1–3, pp. 401–409, 2008.

[23] O. V. Yakubovich and V. V. Kirrev, "Refinement of the crystal structure of $Na_2Ti_3O_7$," *Crystallography Reports*, vol. 48, pp. 24–28, 2003.

[24] A. L. Sauvet, S. Baliteau, C. Lopez, and P. Fabry, "Synthesis and characterization of sodium titanates $Na_2Ti_{\ 3}O_7$ and $Na_2Ti_6O_{13}$," *Journal of Solid State Chemistry*, vol. 177, no. 12, pp. 4508–4515, 2004.

[25] M. Qamar, C. R. Yoon, H. J. Oh et al., "Preparation and photocatalytic activity of nanotubes obtained from titanium dioxide," *Catalysis Today*, vol. 131, no. 1–4, pp. 3–14, 2008.

[26] H. F. Yu, Z. W. Zhang, and F.C. Hu, "Phase stabilities and photocatalytic activities of P/ZN-TiO_2 nanoparticles able to operate under uv-vis light irradiation," *Journal of Alloys and Compounds*, vol. 465, pp. 484–490, 2008.

[27] Y. Chen, J. C. Crittenden, S. Hackney, L. Sutter, and D. W. Hand, "Preparation of a novel TiO_2-based p-n junction nanotube photocatalyst," *Environmental Science and Technology*, vol. 39, no. 5, pp. 1201–1208, 2005.

[28] G. K. Mor, O. K. Varghese, M. Paulose, K. Shankar, and C. A. Grimes, "A review on highly ordered, vertically oriented TiO_2 nanotube arrays: fabrication, material properties, and solar energy applications," *Solar Energy Materials and Solar Cells*, vol. 90, no. 14, pp. 2011–2075, 2006.

[29] H. C. Choi, Y. M. Jung, and S. B. Kim, "Size effects in the Raman spectra of TiO_2 nanoparticles," *Vibrational Spectroscopy*, vol. 37, no. 1, pp. 33–38, 2005.

[30] T. Ohsaka, F. Izumi, and Y. Fujiki, "Raman spectrum of anatase, TiO_2," *Journal of Raman Spectroscopy*, vol. 7, pp. 321–324, 1978.

[31] H. Berger, H. Tang, and F. Levy, "Growth and Raman spectroscopic characterization of TiO_2 anatase single crystals," *Journal of Crystal Growth*, vol. 130, pp. 108–112, 1993.

[32] Z. Tang, L. Zhou, L. Yang, and F. Wang, "A study on the structure transformation and luminescence of Eu(III) titanate nanotubes synthesized at various hydrothermal temperatures," *Journal of Alloys and Compounds*, vol. 481, no. 1-2, pp. 704–709, 2009.

[33] R. Ma, K. Fukuda, T. Sasaki, M. Osada, and Y. Bando, "Structural features of titanate nanotubes/nanobelts revealed by raman, X-ray absorption fine structure and electron diffraction characterizations," *Journal of Physical Chemistry B*, vol. 109, no. 13, pp. 6210–6214, 2005.

[34] C. K. Lee, C. C. Wang, M. D. Lyu, L. C. Juang, S. S. Liu, and S. H. Hung, "Effects of sodium content and calcination temperature on the morphology, structure and photocatalytic activity of nanotubular titanates," *Journal of Colloid and Interface Science*, vol. 316, no. 2, pp. 562–569, 2007.

[35] G. S. Kim, Y. S. Kim, H. K. Seo, and H. S. Shin, "Hydrothermal synthesis of titanate nanotubes followed by electrodeposition process," *Korean Journal of Chemical Engineering*, vol. 23, no. 6, pp. 1037–1045, 2006.